Analysis of Axisymmetrical Shells by the Direct Stiffness Method

PETER E. GRAFTON* AND DONALD R. STROME†
The Boeing Company, Seattle, Wash.

A method for the structural analysis of shells of revolution, composed of materials with orthotropic properties, is discussed. The development is based on the direct stiffness method. A truncated cone element is introduced to take advantage of symmetry. Derivations of the stiffness and stress matrices for the truncated cone element are given. Several examples are solved on the digital computing machine using a program that is based on the truncated cone element. The results are compared to other theoretical results, and the correlation is excellent. Extension of the technique to handle linear unsymmetric deformation and nonlinear symmetric deformation is discussed.

Nomenclature

E	=	modulus of elasticity
F	=	generalized force
k,K	=	stiffness coefficient
l	=	length of element along meridian
r	=	radius of nodal line
S	=	stress coefficient
T,N,M	=	forces and moments per unit length along nodal line
t	=	thickness
U	=	strain energy in element
u,w,β	=	displacements and rotation at nodal lines
δ	=	generalized displacement
σ	=	generalized stress resultant
ϵ	=	strain
ν	=	Poisson's ratio
ϕ	=	angle between axis of revolution and tangent to meridian
$\{\ \}$	=	column matrix
$[\ ]$	=	square matrix
$\|\|\|$	=	rectangular matrix

Subscript

L	=	longitudinal direction
C	=	circumferential direction
1	=	nodal line one
2	=	nodal line two

Introduction

PRESSURE vessels have been a type of shell structure of considerable practical interest for some time. The structures engineer has been concerned with the ability to predict stresses and deformations occurring in them, for purposes of assuring structural integrity. Two developments have resulted in additional emphasis on the ability to do this. One is the striving for high structural efficiency in aerospace applications, requiring distribution of structural material for optimum performance. Perhaps more important has been the advent of new structural materials such as filament wound Fiberglas, which permits this distribution to be accomplished by tailoring both elastic and strength properties to meet the needs of a specific application. However, this cannot be accomplished unless the engineer is able to predict the stress and deformation behavior of a given configuration and loading.

It is the purpose of this paper to present the development of analysis techniques for a common type of pressure vessel, the shell of revolution, with capability of accounting for the orthotropic elastic properties encountered in filament wound Fiberglas shells. The development is based on techniques which have proved useful in the analysis of complex redundant structures, and which are readily automated by use of a digital computer. Based on the direct stiffness approach[1] to the formulation of stress and deformation problems, these techniques have been applied directly to the analysis of isotropic shell structures.[2] For shells of revolution with axisymmetric loading, the modifications developed here, which take advantage of rotational symmetry, offer significant savings in the time and labor of analysis.

This paper is organized to provide initially a summary review of the direct stiffness techniques, followed by the modifications involved in applying them to shells of revolution. The development of the required stiffness and stress matrices for the basic element is then outlined. The application of the technique for some simple examples is shown in order to demonstrate accuracy achieved and the utility of the analysis techniques.

Direct Stiffness Method

The direct stiffness method was developed to meet the needs for analysis of complex structures, composed of beams, plates, rods, etc., too complicated to be handled either by simple engineering techniques (such as beam theory) or the classical continuum mechanics approach. It is based on the concept that the actual structure can be idealized as a set of finite elements connecting nodal points. It is assumed that the displacements everywhere in the structure can be described in terms of the displacements of these nodal points, and the actual loading of the structure can be replaced by a set of equivalent loads at the nodal points (equivalent in the sense that the work done during any incremental deformation approximates the work done by the actual loading). Compatibility of deformation is satisfied precisely only at the nodal points and approximately along other element boundaries.

For each element, relationships can be derived, based on the elastic properties of the element and reasonable approximation of the interior deformation of the element, giving the forces at the node points (equivalent to the distributed forces on the element boundaries) in terms of the displacements at the node points. These algebraic equations, written in matrix form are

$$\{F\} = [k]\{\delta\} \tag{1}$$

where $\{F\}$ and $\{\delta\}$ are column matrices of forces and displacements at the nodes, and $[k]$ is the stiffness matrix for the element. For the entire structure, the total stiffness matrix is obtained by superposition (addition) of each of the element stiffness matrices. The force-displacement relation for the entire structure is then

$$\{F\} = [K]\{\delta\} \tag{2}$$

Received March 26, 1963; revision received July 26, 1963.

* Chief, Structural Research and Development, Aero-Space Division. Member AIAA.
† Research Engineer, Aero-Space Division.

where $[K]$ is the total stiffness matrix. This matrix is singular and cannot be inverted. However, the set of Eqs. (2) can be arranged and partitioned so that

$$\left\{\begin{matrix} F \\ R \end{matrix}\right\} = \left[\begin{matrix} K_{11} & K_{12} \\ K_{21} & K_{22} \end{matrix}\right]\left\{\begin{matrix} \delta \\ C \end{matrix}\right\} \tag{3}$$

where $\{F\}$ are the specified loads applied to the structure, $\{R\}$ are the (unknown) reactions at points of support or constrained deflections, $\{\delta\}$ are the (unknown) displacements, and $\{C\}$ are the specified displacements (zero in many cases) of the support points. For kinematically stable structures, the reduced stiffness matrix $[K_{11}]$ is nonsingular and can be inverted. This permits solution for the unknown displacements and reactions:

$$\begin{aligned} \{\delta\} &= [K_{11}]^{-1}(\{F\} - [K_{12}]\{C\}) \\ \{R\} &= [K_{21}]\{\delta\} + [K_{22}]\{C\} \end{aligned} \tag{4}$$

where $[K_{11}]^{-1}$ is the inverse of the reduced stiffness matrix. Stresses (or internal loads) in each element can be similarly determined, based on elastic properties and deformation pattern, and found from the nodal displacements:

$$\{\sigma\} = \|S\|\{\delta\} \tag{5}$$

where $\|S\|$ is the stress matrix for the elements. These can be compiled for the entire structure and stresses determined once the displacements have been found.

Implementation of this approach requires the derivation of appropriate stiffness and stress matrices for each type of element to be used and the development of a digital computer program for accomplishing the numerical computations involved in the forementioned operations. This has been accomplished and the technique applied to a variety of structural problems. The effect of temperature gradients can be included by simple modifications, and use of incremental load application permits application to problems where geometric nonlinear effects are important.[3,4] The current status of developments of this technique is summarized in Ref. 5.

Application to Shells of Revolution

The principal changes involved in applying this technique to shells of revolution with rotationally symmetric loading are a change in nodal concept and the development of stiffness and stress matrices for a different type of element. The nodal points previously used are replaced by nodal circles on the shell as shown in Fig. 1. The displacements of the shell can then be approximated from three components of displacement (two components of linear displacement and a rotation) at each nodal point, u_i, w_i, and β_i, as shown in Fig. 1. The corresponding equivalent loading (two force components and a moment, T_i, N_i, and M_i) are also shown. These are distributed around the circumference of the shell. The prime advantage of this modification, taking advantage of rotational symmetry, is the replacement of a large number of nodal points, each having six degrees-of-freedom in the general case, by a relatively smaller number of nodal circles, each having three degrees-of-freedom. The saving in size of matrices to be manipulated is obvious.

Use of the circular nodes requires use of a different structural element, the segment of shell between two adjacent nodes. Various degrees of refinement in approximating the geometry of the segment are possible; the one used here is the short truncated cone as shown in Fig. 1, which combines acceptable accuracy with relative simplicity of results for programming. This type of approximation has been used in previous analysis.[6] The details of derivation of the stiffness and stress matrices for this element are outlined in the paper. In order to permit the use of this technique for analysis of shells with variable and orthotropic elastic properties, the derivation includes these effects. The derivation also provides a basis for determining the equivalent applied nodal forces in the case of pressure loading.

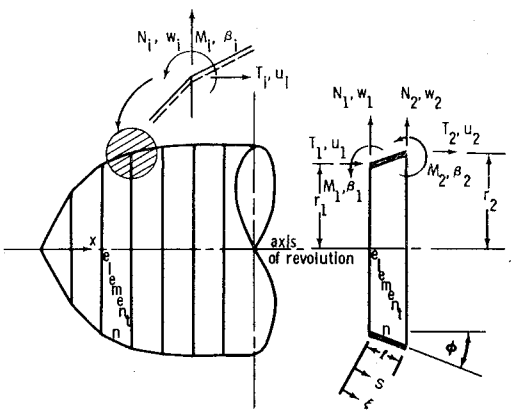

Fig. 1 Idealization of shell by truncated cone element.

The end closure element of a complete shell requires a special consideration. Either a complete shallow cone or a circular flat plate element would be compatible with the forementioned general element. Whereas the shallow cone is presently programmed and is used in the examples to follow, it offers no particular advantage over the simpler flat plate.

Stiffness Matrix

A direct method for determining the stiffness matrix of a structural element is to use the relationship between the strain energy in an element and the stiffness coefficients as derived in Ref. 2. This relationship is

$$k_{ij} = \partial^2 U/\partial\delta_i\partial\delta_j \tag{6}$$

where U is the strain energy in the element, and δ's are the displacements at the nodes. The strain energy is determined by assuming an arbitrary deformed shape and stress-strain functions.

A set of displacement functions which satisfy the end conditions and the relationship between the change in slope and displacements, i.e.,

$$\beta = (dw/ds)\cos\phi - (du/ds)\sin\phi \tag{7}$$

can be written as

$$\begin{aligned} u &= (1-\xi)u_1 + \xi u_2 - (\xi - 2\xi^2 + \xi^3)[\beta_1 l + (u_2 - u_1)\sin\phi - (w_2 - w_1)\cos\phi]\sin\phi + \\ &\quad \xi^2(1-\xi)[\beta_2 l + (u_2 - u_1)\sin\phi - (w_2 - w_1)\cos\phi]\sin\phi \\ w &= (1-\xi)w_1 + \xi w_2 + (\xi - 2\xi^2 + \xi^3) \times \\ &\quad [\beta_1 l + (u_2 - u_1)\sin\phi - (w_2 - w_1)\cos\phi]\cos\phi - \\ &\quad \xi^2(1-\xi)[\beta_2 l + (u_2 - u_1)\sin\phi - (w_2 - w_1)\cos\phi]\cos\phi \end{aligned} \tag{8}$$

where $\xi = s/l$. These displacement functions were chosen because they are the simplest functions that satisfy all end conditions for the element. The stress-strain relationships for an orthotropic material are

$$N_L = C_L\epsilon_L + C_{LC}\epsilon_C \qquad N_C = C_{CL}\epsilon_L + C_C\epsilon_C \tag{9}$$

where

$$C_L = \frac{E_L t}{1 - \nu_{LC}\nu_{CL}} \qquad C_C = \frac{E_C t}{1 - \nu_{LC}\nu_{CL}}$$

$$C_{LC} = C_{CL} = \nu_{LC}C_C = \nu_{CL}C_L \tag{10}‡$$

Relationships between bending moments and curvature are

$$M_L = D_L\chi_L + D_{LC}\chi_C \qquad M_C = D_{CL}\chi_L + D_C\chi_C \tag{11}$$

‡ The modulus of elasticity and Poisson's ratio may have different values in Eqs. (10) and (12). The material may have different stiffness values for membrane and bending effects.

where

$$D_L = \frac{E_L t^3}{12(1 - \nu_{LC}\nu_{CL})} \qquad D_C = \frac{E_C t^3}{12(1 - \nu_{LC}\nu_{CL})} \tag{12}$$

$$D_{LC} = D_{CL} = \nu_{LC} D_C = \nu_{CL} D_L$$

The following equations are also applicable:

$$\epsilon_L = (du/ds)\cos\phi + (dw/ds)\sin\phi \qquad \epsilon_C = w/r \tag{13}$$

$$\chi_L = d\beta/ds \qquad \chi_C = (\beta/r)\sin\phi$$

The strain energy U in the element is

$$U = \tfrac{1}{2}\int 2\pi r(N_L\epsilon_L + N_C\epsilon_C + M_L\chi_L + M_C\chi_C)ds \tag{14}$$

Using Eqs. (7–13) and assuming the integrand in Eq. (14) is linear in ξ, U may be written

$$\begin{aligned} U = (\pi l/2)\{&r_1(C_{L1}\epsilon_{L1}^2 + C_{C1}\epsilon_{C1}^2 + 2C_{LC1}\epsilon_{L1}\epsilon_{C1} + \\ &D_{L1}\chi_{L1}^2 + D_{C1}\chi_{C1}^2 + 2D_{LC1}\chi_{L1}\chi_{C1}) + \\ &r_2(C_{L2}\epsilon_{L2}^2 + C_{C2}\epsilon_{C2}^2 + 2C_{LC2}\epsilon_{L2}\epsilon_{C2} + \\ &D_{L2}\chi_{L2}^2 + D_{C2}\chi_{C2}^2 + 2D_{CL2}\chi_{L2}\chi_{C2})\} \end{aligned} \tag{15}$$

The stiffness elements are determined from Eq. (6). Force displacement relationship for a truncated cone element is

$$[A]\begin{Bmatrix} T_1 \\ N_1 \\ M_1 \\ T_2 \\ N_2 \\ M_2 \end{Bmatrix} = [k]\begin{Bmatrix} u_1 \\ w_1 \\ \beta_1 \\ u_2 \\ w_2 \\ \beta_2 \end{Bmatrix} \tag{16}$$

In order to insure $[k]$ being symmetric, the forces $\{F\}$ shown in Fig. 1 are premultiplied by a diagonal matrix $[A]$ to convert them from load per unit length of the circumference to total load at a nodal line:

$$\text{matrix } [A] = \begin{bmatrix} 2\pi r_1 & & & & & \\ 0 & 2\pi r_1 & & & \text{symmetric} & \\ 0 & 0 & 2\pi r_1 & & & \\ 0 & 0 & 0 & 2\pi r_2 & & \\ 0 & 0 & 0 & 0 & 2\pi r_2 & \\ 0 & 0 & 0 & 0 & 0 & 2\pi r_2 \end{bmatrix} \tag{17}$$

The stiffness coefficients k_{ij} are listed below:

$$\begin{aligned}
k_{11} &= (\pi/l)\{(r_1C_{L1} + r_2C_{L2})\cos^2\phi + (36/l^2)(r_1D_{L1} + r_2D_{L2})\sin^2\phi\} \\
k_{12} &= k_{21} = -k_{24} = -k_{42} = (\pi/l)\cos\phi\{(r_1C_{L1} + r_2C_{L2})\sin\phi - lC_{LC1} - (36/l^2)(r_1D_{L1} + r_2D_{L2})\sin\phi\} \\
k_{13} &= k_{31} = -k_{34} = -k_{43} = -(6\pi\sin\phi/l^2)\{2(2r_1D_{L1} + r_2D_{L2}) - lD_{LC1}\sin\phi\} \\
k_{14} &= k_{41} = -k_{11} = k_{44} \\
k_{15} &= k_{51} = -k_{45} = -k_{54} = -(\pi/l)\cos\phi\{(r_1C_{L1} + r_2C_{L2})\sin\phi + lC_{LC2} - (36/l^2)(r_1D_{L1} + r_2D_{L2})\sin\phi\} \\
k_{16} &= k_{61} = -k_{46} = -k_{64} = -(6\pi\sin\phi/l^2)\{2(r_1D_{L1} + 2r_2D_{L2}) + lD_{LC2}\sin\phi\} \\
k_{22} &= (\pi/l)\{(r_1C_{L1} + r_2C_{L2})\sin^2\phi - 2lC_{LC1}\sin\phi + (l^2/r_1)C_{C1} + (36/l^2)(r_1D_{L1} + r_2D_{L2})\cos^2\phi\} \\
k_{23} &= k_{32} = -k_{35} = -k_{53} = (6\pi\cos\phi/l^2)\{2(2r_1D_{L1} + r_2D_{L2}) - lD_{LC1}\sin\phi\} \\
k_{25} &= k_{52} = -(\pi/l)\{(r_1C_{L1} + r_2C_{L2})\sin^2\phi - l(C_{LC1} - C_{LC2})\sin\phi + (36/l^2)(r_1D_{L1} + r_2D_{L2})\cos^2\phi\} \\
k_{26} &= k_{62} = (6\pi\cos\phi/l^2)\{2(r_1D_{L1} + 2r_2D_{L2}) + lD_{LC2}\sin\phi\} \\
k_{33} &= (4\pi/l)\{(4r_1D_{L1} + r_2D_{L2}) - 2lD_{LC1}\sin\phi + (l^2/4r_1)D_{C1}\sin^2\phi\} \\
k_{36} &= k_{63} = (2\pi/l)\{4(r_1D_{L1} + r_2D_{L2}) - l(D_{LC1} - D_{LC2})\sin\phi\} \\
k_{55} &= (\pi/l)\{(r_1C_{L1} + r_2C_{L2})\sin^2\phi + 2lC_{LC2}\sin\phi + l^2/r_2C_{C2} + (36/l^2)(r_1D_{L1} + r_2D_{L2})\cos^2\phi\} \\
k_{56} &= k_{65} = -(6\pi\cos\phi/l^2)\{2(r_1D_{L1} + 2r_2D_{L2}) + lD_{LC2}\sin\phi\} \\
k_{66} &= (\pi/l)\{4(r_1D_{L1} + 4r_2D_{L2}) + 8lD_{LC2}\sin\phi + (l^2/r_2)D_{C2}\sin^2\phi\}
\end{aligned} \tag{18}$$

Stress Matrix

The stiffness matrix $[K]$ for the entire structure is obtained by merging the stiffness matrix $[k]$ for the individual elements. Deflections are then determined from Eq. (4). Equation (5) relates the stresses to the deflections of the nodal lines through a stress matrix. The stress matrix $[S]$ is written as follows:

$$[S] = [A]^{-1}[k] \tag{19}$$

Stress resultants, not stresses, are computed, these generally being the quantities of interest. The matrix $[A]^{-1}$ insures that the loads are per unit length of circumference, therefore true stress resultants.

It is of interest to have stress resultants in the circumferential direction computed for the truncated cone element. By manipulating Eqs. (9–13), these circumferential stress resultants may be written

$$\begin{Bmatrix} N_{C1} \\ M_{C1} \\ N_{C2} \\ M_{C2} \end{Bmatrix} = \|\bar{S}\|\begin{Bmatrix} u_1 \\ w_1 \\ \beta_1 \\ u_2 \\ w_2 \\ \beta_2 \end{Bmatrix} \tag{20}$$

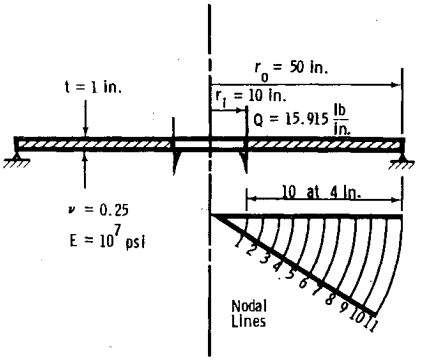

Fig. 2 Circular plate, properties and nodal breakdown.

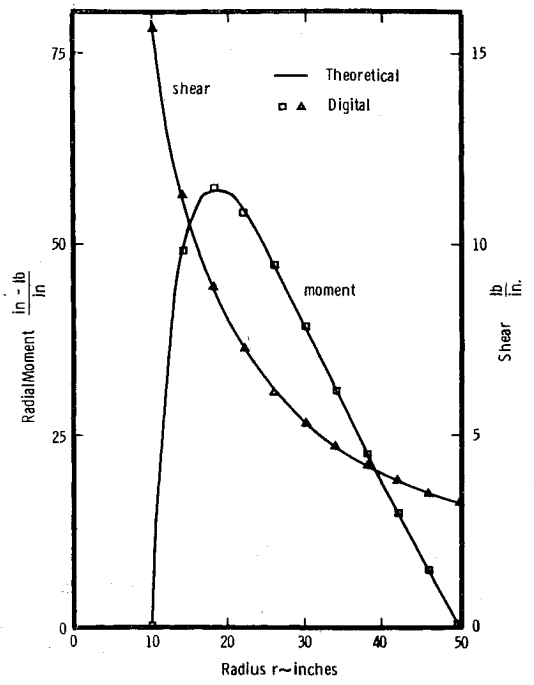

Fig. 3 Stress resultants, circular plate.

The stress $\|\bar{S}\|$ is listed below:

$$\left\|\begin{array}{cccccc}
-\frac{C_{LC1}}{l}\cos\phi & \frac{C_{C1}}{r_1}-\frac{C_{LC1}}{l}\sin\phi & 0 & \frac{C_{LC1}}{l}\cos\phi & \frac{C_{LC1}}{l}\sin\phi & 0 \\
\frac{6D_{LC1}}{l^2}\sin\phi & -\frac{6D_{LC1}}{l^2}\cos\phi & -\frac{4D_{LC1}}{l}+\frac{D_{C1}}{r_1}\sin\phi & -\frac{6D_{LC1}}{l^2}\sin\phi & \frac{6D_{LC1}}{l^2}\cos\phi & -\frac{D_{LC1}}{l} \\
-\frac{C_{LC2}}{l}\cos\phi & -\frac{C_{LC2}}{l}\sin\phi & 0 & \frac{C_{LC2}}{l}\cos\phi & \frac{C_{C2}}{r_2}+\frac{C_{LC2}}{l}\sin\phi & 0 \\
-\frac{6D_{LC2}}{l^2}\sin\phi & \frac{6D_{LC2}}{l^2}\cos\phi & \frac{2D_{LC2}}{l} & \frac{6D_{LC2}}{l^2}\sin\phi & -\frac{6D_{LC2}}{l^2}\cos\phi & \frac{4D_{LC2}}{l}+\frac{D_{C2}}{r_2}\sin\phi
\end{array}\right\|$$

Linear Unsymmetric Deformation

The truncated cone element may be used to solve for displacements and stresses in a shell of revolution subjected to unsymmetric loadings. For the unsymmetric case the stiffness matrix for the element becomes an 8×8, whereas in the symmetric case a 6×6 was sufficient. The unsymmetric loading case introduces a shear flow and displacement in the circumferential direction, which adds a row and column to the stiffness matrix at each nodal line of the truncated cone element.

The displacements of the shell element are written in a Fourier series such as

$$\begin{aligned} u &= u(\xi)\Sigma\cos n\theta \qquad & w &= w(\xi)\Sigma\cos n\theta \\ \beta &= \beta(\xi)\Sigma\cos n\theta \qquad & v &= v(\xi)\Sigma\sin n\theta \end{aligned} \tag{21}$$

where v represents the displacement in the circumferential direction. The stiffness matrix can be generated assuming stress-strain relationships along with the displacements given by Eqs. (21). This stiffness matrix will be a function of n and may be written as

$$[K] = [K]_{n=0} + [K]_{n=1} + \ldots \tag{22}$$

Loads acting on the structure may also be written in Fourier series form:

$$\begin{aligned} T &= \Sigma T_n\cos n\theta \qquad & N &= \Sigma N_n\cos n\theta \\ M &= \Sigma M_n\cos n\theta \qquad & Q &= \Sigma Q_n\sin n\theta \end{aligned} \tag{23}$$

where Q is the shear force in the circumferential direction.

The term $n = 0$ corresponds to the symmetric case that was discussed in the paper. The solution to the general unsymmetrical case consists of writing the applied loads in Fourier series form and determining the displacements for each term in the series:

$$\begin{aligned} \{F\}_{n=0} &= [K]_{n=0}\{\delta\}_{n=0} \\ \{F\}_{n=1} &= [K]_{n=1}\{\delta\}_{n=1}, \text{ etc.} \end{aligned} \tag{24}$$

For each value of n, the stiffness matrices for the individual elements are merged and deflections are computed as outlined previously in the paper for $n = 0$. Displacements are determined by summing the component displacements corresponding to $n = 0, 1 \ldots n$, since linearity was assumed. This procedure obviously becomes involved if n is required to be large to represent adequately the loading by a Fourier series.

Nonlinear Symmetric Deformation

The stiffness and stress matrices developed for the truncated cone element are based on orthotropic properties of the material. This element, therefore, should be useful in the analysis of Fiberglas shells. For these and other thin shells, which suffer large deformation, nonlinear effects may be of importance.

References (4) and (5) discuss the solution to problems in which the structure behaves nonlinearly. The procedure used consists of a step-by-step piecewise linear analysis. The loads are applied in increments sufficiently small such that during the increment the stiffness matrix is essentially constant. Thus the assumption (that deformations, strains, and rotations have a negligible effect on a change of $[K]$) made in the classical linear theory is also made in the step-by-step piecewise linear analysis.

It was shown in Ref. 2 that

$$k_{ij} = \partial^2 U/\partial\delta_i\partial\delta_j \tag{25}$$

is valid for any deformed shape as long as the strain energy is expressed in terms of this shape and the structure is elastic.

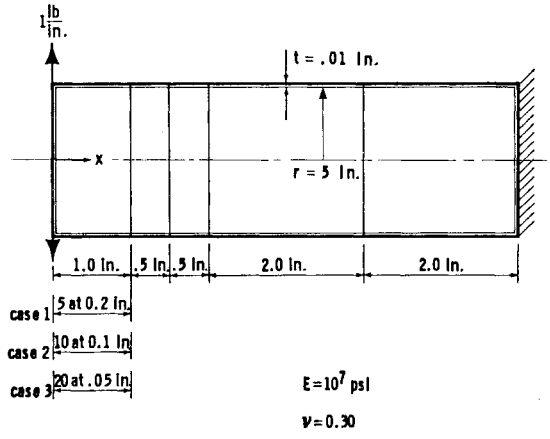

Fig. 4 Cylinder shell, properties and nodal breakdown.

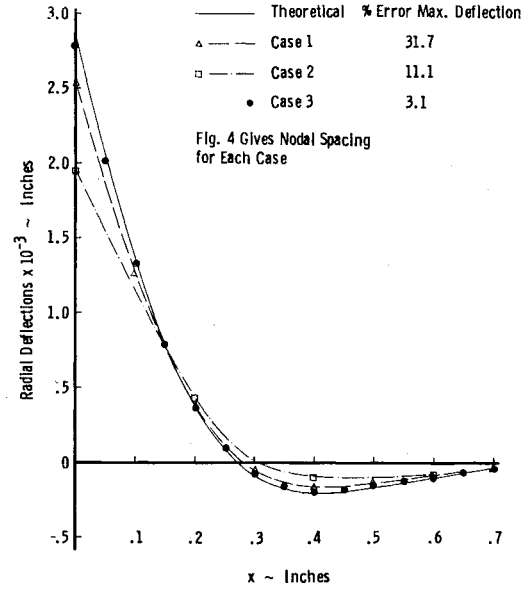

Fig. 5 Displacements, cylindrical shell.

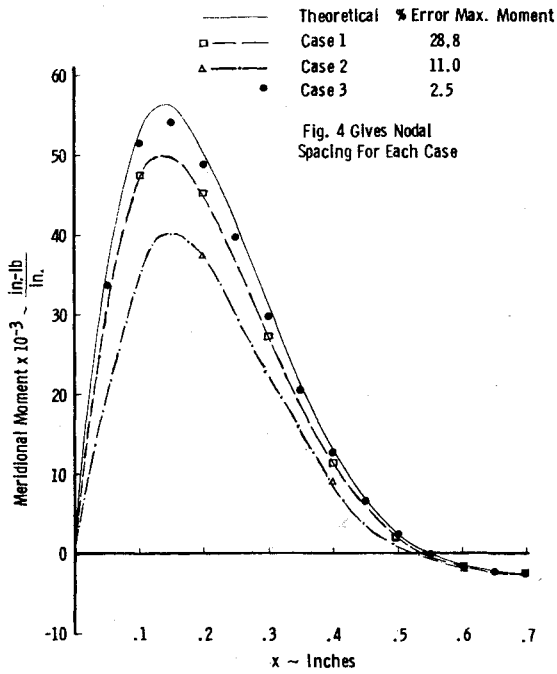

Fig. 6 Meridional moment, cylindrical shell.

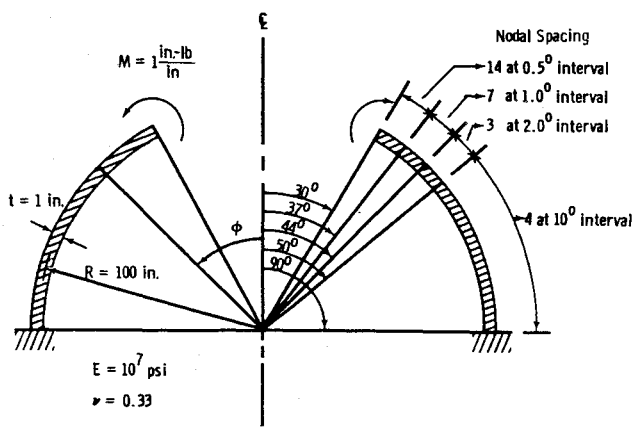

Fig. 7 Hemispherical shell, properties and nodal breakdown.

This stiffness rate relates the increment of force to displacement such that

$$\{\Delta F_1\} = [K]\{\Delta\delta_1\} \tag{26}$$

At each incremental change in shape the stiffness matrix is recalculated. The final displacements are the sum of the incremental deformations. In Refs. 4 and 5 a procedure is discussed where the step-by-step analysis is automatically performed on a digital computer.

Conclusions

The direct stiffness method has proven to be a very powerful tool in the structural analysis of complex structures. This paper presents a new concept of nodal lines replacing the node points and gives illustrations of its use for shells of revolutions.

The examples discussed in the paper show the excellent agreement between theory and computed points determined by the direct stiffness method based on the truncated cone elements. Except for the Fiberglas joint problem, the examples given are based on isotropic material properties for ease in computing theoretical solutions. The important use of the program, though, is for structures made of material having orthotropic properties. No difficulty is experienced with these materials if the properties are known or can be determined. Input, time-to-run, and output are the same whether the material has isotropic or orthotropic properties.

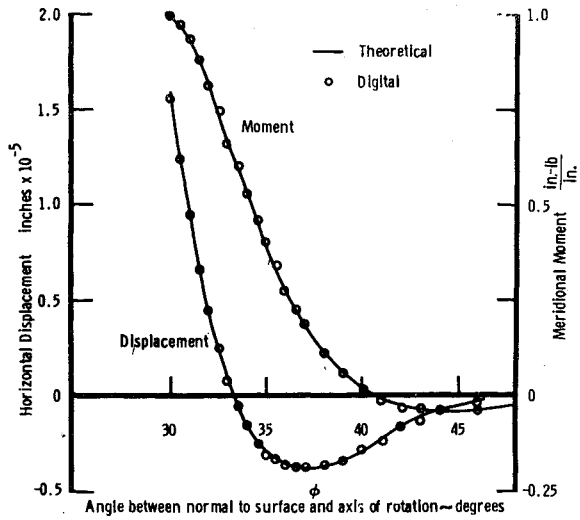

Fig. 8 Stress resultant and displacement, hemispherical shell.

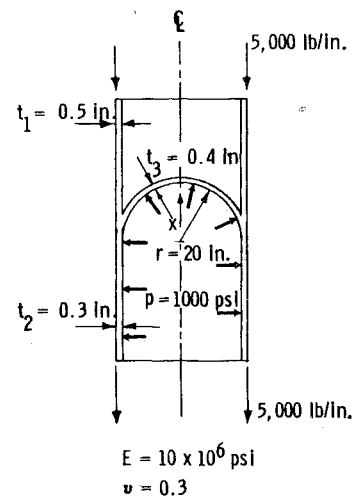

Fig. 9 Head-cylinder-skirt junction.

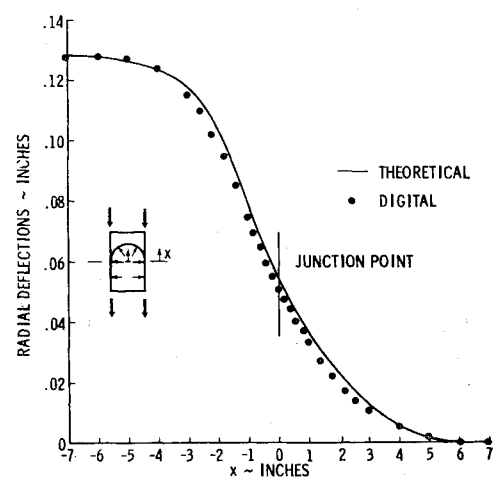

Fig. 10 Radial deflections along direction of cylinder axis near junction point.

Examples

Three examples are shown in Figs. 2–8 demonstrating the accuracy of the direct stiffness method based on the truncated

Table 1 Input data for example shown in Fig. 11

Nodal line	x, in.	r, in.	t, in.	Membrane stiffness E_L, psi	Membrane stiffness E_C, psi	Bending stiffness E_L, psi	Bending stiffness E_C, psi	ν_{LC}	ν_{CL}
1	0	9.13	0.54	17.38×10^6	17.85×10^6	23.07×10^6	23.31×10^6	0.24	0.25
2	0.32	9.13	0.54	17.38×10^6	17.85×10^6	23.07×10^6	23.31×10^6	0.24	0.25
3	0.64	9.13	0.54	17.38×10^6	17.85×10^6	23.07×10^6	23.31×10^6	0.24	0.25
4	0.96	9.13	0.54	17.38×10^6	17.85×10^6	23.07×10^6	23.31×10^6	0.24	0.25
5	1.28	9.13	0.54	17.38×10^6	17.85×10^6	23.07×10^6	23.31×10^6	0.24	0.25
6	1.60	9.13	0.54	17.38×10^6	17.85×10^6	23.07×10^6	23.31×10^6	0.24	0.25
7	1.80	9.13	0.38	12.08×10^6	12.67×10^6	9.86×10^6	10.57×10^6	0.20	0.22
8	2.0	9.13	0.38	12.08×10^6	12.67×10^6	9.86×10^6	10.57×10^6	0.20	0.22
9	2.20	9.13	0.38	12.08×10^6	12.67×10^6	9.86×10^6	10.57×10^6	0.20	0.22
10	2.40	9.13	0.38	12.08×10^6	12.67×10^6	9.86×10^6	10.57×10^6	0.20	0.22
11	2.60	9.13	0.38	12.08×10^6	12.67×10^6	9.86×10^6	10.57×10^6	0.20	0.22
12	2.80	9.10	0.35	10.71×10^6	11.43×10^6	7.32×10^6	8.10×10^6	0.19	0.21
13	3.00	9.07	0.33	9.23×10^6	10.0×10^6	5.34×10^6	6.28×10^6	0.18	0.20
14	3.20	9.07	0.33	9.23×10^6	10.0×10^6	5.34×10^6	6.28×10^6	0.18	0.20
15	3.50	9.05	0.30	7.50×10^6	8.33×10^6	4.16×10^6	5.06×10^6	0.17	0.19
16	3.80	9.05	0.30	7.50×10^6	8.33×10^6	4.16×10^6	5.06×10^6	0.17	0.19
17	4.10	9.05	0.30	7.50×10^6	8.33×10^6	4.16×10^6	5.06×10^6	0.17	0.19
18	4.40	9.04	0.28	5.45×10^6	6.36×10^6	3.80×10^6	4.84×10^6	0.16	0.19
19	4.70	9.04	0.28	5.45×10^6	6.36×10^6	3.80×10^6	4.84×10^6	0.16	0.19
20	5.00	9.04	0.28	5.45×10^6	6.36×10^6	3.80×10^6	4.84×10^6	0.16	0.19
21	5.40	9.04	0.28	5.45×10^6	6.36×10^6	3.80×10^6	4.84×10^6	0.16	0.19
22	6.15	9.07	0.25	3.00×10^6	4.00×10^6	3.00×10^6	4.00×10^6	0.075	0.10
23	6.90	9.07	0.25	3.00×10^6	4.00×10^6	3.00×10^6	4.00×10^6	0.075	0.10
24	7.65	9.07	0.25	3.00×10^6	4.00×10^6	3.00×10^6	4.00×10^6	0.075	0.10
25	8.40	9.07	0.25	3.00×10^6	4.00×10^6	3.00×10^6	4.00×10^6	0.075	0.10
26	9.15	9.07	0.25	3.00×10^6	4.00×10^6	3.00×10^6	4.00×10^6	0.075	0.10
27	11.15	9.07	0.25	3.00×10^6	4.00×10^6	3.00×10^6	4.00×10^6	0.075	0.10
28	13.15	9.07	0.25	3.00×10^6	4.00×10^6	3.00×10^6	4.00×10^6	0.075	0.10
29	15.15	9.07	0.25	3.00×10^6	4.00×10^6	3.00×10^6	4.00×10^6	0.075	0.10

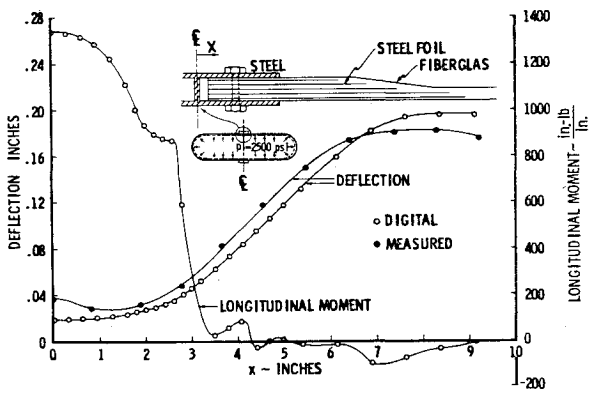

Fig. 11 Radial deflection and longitudinal moment variation near joint in Fiberglas pressure vessel.

cone element. The problems all had rapidly varying stress resultants and deflections, which were followed very accurately by the digital program. Examples were chosen to show agreement between theory and digital results based on the truncated cone element for structures ranging from a flat circular plate to a doubly curved spherical shell. Computing times for these examples were less than 1 min.

Figure 9 is a typical joint in a missile in which the shells are pressurized and also carry thrust loads. Example is solved using isotropic properties for ease in solving for theoretical answers, but the technique can just as easily be applied to problems if materials have orthotropic properties. Deflections are shown in Fig. 10.

Figure 11 shows a typical joint used in Fiberglas construction. In order to test the joint, it was formed in a Fiberglas pressure vessel by cutting through the center of the tank. The joint consisted of an elongated I section with steel shims imbedded in the Fiberglas rovings. Excellent agreement between digital computed results and experimental points is shown. Table 1 gives the material and geometric properties used in the digital program.

References

[1] Turner, M. J., Clough, R. W., Martin, H. C., and Topp, L. J., "Stiffness and deflection analysis of complex structures," J. Aeronaut. Sci. **23**, 805–824 (1956).

[2] Greene, B. E., Strome, D. R., and Weikel, R. C., "Application of the stiffness method to the analysis of shell structures," Am. Soc. Mech. Engrs. Paper 61-AV-58 (1961).

[3] Turner, M. J., Dill, E. H., Martin, H. C., and Melosh, R. J., "Large deflections of structures subjected to heating and external loads," J. Aerospace Sci. **27**, 97–107 (1960).

[4] Weikel, R. C., Jones, R. E., Seiler, J. A., Martin, H. C., and Greene, B. E., "Nonlinear and thermal effects on elastic vibrations," Aeronaut. Systems Div. ASD-TDR-62-156 (1962).

[5] Turner, M. J., Martin, H. C., and Weikel, R. C., "Further development and applications of the stiffness method," presented at the AGARD Structures and Materials Panel in Paris, France on July 6, 1962; available also as Boeing Document no. D2-22061.

[6] Meyer, R. R. and Harmon, M. B., "Conical segment method for analyzing open crown shells of revolution for edge loading," AIAA J. **1**, 886–891 (1963).